OsAGO2 controls ROS production and the initiation of tapetal PCD by epigenetically regulating *OsHXK1* expression in rice anthers

Shaoyan Zheng[a,b,c,1], Jing Li[a,b,c,1], Lu Ma[a,b,c], Hailong Wang[a,b,c], Hai Zhou[a,b,c], Erdong Ni[a,b,c], Dagang Jiang[a,b,c], Zhenlan Liu[a,b,c], and Chuxiong Zhuang[a,b,c,2]

[a]State Key Laboratory for Conservation and Utilization of Subtropical Agro-Bioresources, South China Agricultural University, 510642 Guangzhou, China; [b]Key Laboratory of Plant Functional Genomics and Biotechnology of Guangdong Provincial Higher Education Institutions, South China Agricultural University, 510642 Guangzhou, China; and [c]College of Life Sciences, South China Agricultural University, 510642 Guangzhou, China

Edited by David C. Baulcombe, University of Cambridge, Cambridge, United Kingdom, and approved February 25, 2019 (received for review October 17, 2018)

Proteins of the ARGONAUTE (AGO) family function in the epigenetic regulation of gene expression. Although the rice (*Oryza sativa*) genome encodes 19 predicted AGO proteins, few of their functions have thus far been characterized. Here, we show that the AGO protein OsAGO2 regulates anther development in rice. *OsAGO2* was highly expressed in anthers. Knockdown of *OsAGO2* led to the overaccumulation of reactive oxygen species (ROS) and abnormal anther development, causing premature initiation of tapetal programmed cell death (PCD) and pollen abortion. The expression level of *Hexokinase 1* (*OsHXK1*) increased significantly, and the methylation levels of its promoter decreased, in plants with knocked-down *OsAGO2* expression. Overexpression of *OsHXK1* also resulted in the overaccumulation of ROS, premature initiation of PCD, and pollen abortion. Moreover, knockdown of *OsHXK1* restored pollen fertility in *OsAGO2* knockdown plants. Chromatin immunoprecipitation assays demonstrated that OsAGO2 binds directly to the *OsHXK1* promoter region, suggesting that *OsHXK1* is a target gene of OsAGO2. These results indicate that OsHXK1 controls the appropriate production of ROS and the proper timing of tapetal PCD and is directly regulated by OsAGO2 through epigenetic regulation.

AGO2 | epigenetics | HXK1 | ROS | PCD

Rice (*Oryza sativa* L.) is the staple food for more than half the world's population. It is estimated that rice production will need to increase by ∼30% in 2030 to meet demands (1). Improving grain yield has become an important goal in rice breeding. Grain yield is affected by many genetic and environmental factors, such as pollen fertility and both abiotic and biotic stresses. Among these, pollen fertility is of particular importance. The anther is a portion of the stamen in which pollen grains develop. Rice anthers normally contain four compartments, known as lobes. Abnormal anther development will result in decreased pollen fertility, subsequently reducing yields (2–4). Therefore, improving our understanding of reproductive development (young microspore stage of pollen development) may help increase grain yields and facilitate rice breeding.

Rice anther development is a complex process (5–7) that can be divided into 14 stages according to morphological characteristics, which is consistent with that in *Arabidopsis thaliana* (5, 6, 8, 9). The tapetum, the innermost layer of the anther lobe, is derived from inner secondary parietal cells. The tapetum contributes to microspore release, nutrition, pollen wall synthesis, and pollen coat deposition (7, 10, 11); these functions are essential for pollen development (12). Tapetal cell fate can be divided into three phases: tapetum differentiation, tapetum formation, and apoptosis of tapetal cells. During the late stage of pollen development (stage 8 to stage 10), the tapetum undergoes programmed cell death (PCD). During PCD, tapetum degeneration occurs, along with the loosening of pollen from the surrounding tissue, the release of tapetal remnants, and the deposition of materials onto the pollen coating (13, 14). The excessive production of reactive oxygen species (ROS) in tapetal cells causes oxidative damage to proteins, lipids, and DNA, ultimately resulting in cell death. ROS can trigger PCD, and ROS levels are correlated with the regulation of cell death (15, 16). Timely PCD is critical for pollen development, and maintaining ROS homeostasis is crucial for cell growth and survival during various stages of anther development (6, 17).

The anther and pollen gene regulatory network is a complex system involving gene expression and interactions (8, 9). In recent years, significant progress has been made toward understanding the relationship between the expression of anther or pollen development-related genes and male fertility in *Arabidopsis*. These genes include *DYSFUNCTIONAL TAPETUM1* (*DYT1*), *ABORTED MICROSPORE* (*AMS*), *MALE STERILITY1* (*MS1*), and *MS188/MYB80* (18–24). There is a high degree of conservation

Significance

Understanding the development of anthers, the male reproductive organs of plants, has key implications for crop yield. Epigenetic mechanisms modulate gene expression by altering modifications of DNA or histones and via noncoding RNAs. Many studies have examined anther development, but the involvement of epigenetic mechanisms remains to be explored. Here, we investigated the role of an ARGONAUTE (AGO) family protein, OsAGO2. We find that OsAGO2 epigenetically regulates anther development by modulating DNA methylation modifications in the *Hexokinase* (*OsHXK*) promoter region. OsHXK1, in turn, affects anther development by regulating the production of reactive oxygen and the initiation of cell death in key anther structures. Identification of this epigenetic regulatory mechanism has implications for the production of hybrid crop varieties.

Author contributions: C.Z. designed research; S.Z., L.M., H.W., H.Z., E.N., D.J., and Z.L. performed research; S.Z. and J.L. analyzed data; and S.Z. and J.L. wrote the paper.

The authors declare no conflict of interest.

This article is a PNAS Direct Submission.

Data deposition: Sequence data from this article can be found in the Rice Annotation Project (https://rapdb.dna.affrc.go.jp/viewer/gbrowse) and have been deposited in the GenBank database [Os04g0615700 (*OsAGO2*), Os07g0446800 (*OsHXK1*), and Os10g0510000 (*OsActin1*)]. The tapetal genes deposited in the GenBank database include accession nos. Os07g0549600 (*OsUDT1*), Os01g0293100 (*OsTIP2*), Os02g0120500 (*OsTDR1*), Os04g0599300 (*OsEAT1*), Os04g0470600 (*OsMYB80/OsMYB103*), Os09g0489500 (*OsTGA10*), Os09g0449000 (*OsPTC1*), Os01g0201700 (*OsMADS3*), and Os07g0540366 (*OsDTC1*). The *OsRBOH* genes deposited in the GenBank database include accession nos. Os01g0734200 (*OsRBOHa/OsNOX*), Os01g0360200 (*OsRBOHb*), Os05g0528000 (*OsRBOHc*), Os05g0465800 (*OsRBOHd*), Os01g0835500 (*OsRBOHe*), Os08g0453700 (*OsRBOHf*), Os09g0438000 (*OsRBOHg*), Os12g0541300 (*OsRBOHh*), and Os11g0537400 (*OsRBOHi*).

[1]S.Z. and J.L. contributed equally to this work.

[2]To whom correspondence should be addressed. Email: zhuangcx@scau.edu.cn.

This article contains supporting information online at www.pnas.org/lookup/suppl/doi:10.1073/pnas.1817675116/-/DCSupplemental.

Published online March 22, 2019.

between the networks regulating pollen development in *Arabidopsis* and rice. In rice, diverse regulatory factors with key roles in tapetal PCD and anther development have been identified, including several transcription factors and protein kinases (6). For example, the altered expression of basic helix–loop–helix (bHLH) transcription factor genes has a strong effect on tapetal PCD. These bHLH factors include *Undeveloped Tapetum 1* (*UDT1*/*bHLH164*), *Tapetum Degeneration Retardation 1* (*TDR1*/*bHLH5*), *TDR Interacting Protein 2* (*TIP2*), and *Eternal Tapetum 1* (*EAT1*/*DTD1*/*bHLH141*) (10, 25–29). The MYB transcription factor, *MYB80*/*MYB103*, is involved in tapetal PCD, thereby influencing anther or pollen development (30, 31). The rice MIKC-type MADS box transcription factor, *MADS3*, regulates ROS homeostasis during late anther development (15). Loss-of-function of the PHD finger protein gene, *PERSISTENT TAPETAL CELL1* (*PTC1*), results in complete male sterility (11). In addition, two receptor-like kinases, *DWARF AND RUNTISH SPIKELET1* (*DRUS1*) and *DRUS2*, are involved in regulating PCD and reproductive growth (32).

Epigenetic factors, including DNA methylation, histone modification, and noncoding RNAs, are key regulators of plant development (33). Recent studies have suggested that an increase in global DNA methylation plays a role in tapetal PCD (34). Histone H2B monoubiquitination is another important epigenetic modification that modulates the transcriptional regulation of tapetal PCD in rice (35, 36). Interestingly, noncoding RNAs are also associated with the regulation of tapetal PCD by functioning as posttranscriptional regulators (37). Although epigenetic modifications are essential for tapetal PCD, the underlying regulatory mechanisms remain largely unknown.

Proteins of the ARGONAUTE (AGO) family are major players in the epigenetic regulation of gene expression. Although many functions of AGO proteins have been reported in mammals, little is known about their functions in plants (38). In *Arabidopsis*, the AGO family comprises 10 members (39, 40). Well-studied AGOs—including AGO3, AGO4, AGO6, and AGO9—are responsible for regulating DNA methylation (40–44). Rice contains 19 predicted AGO proteins (45). Among these, AGO18 is required for plant resistance to evolutionarily diverse viruses (46). MEIOSIS ARRESTED AT LEPTOTENE1 (MEL1) epigenetically regulates the meiotic progression of meiocytes and is essential for meiosis (47). In addition, OsAGO4a, OsAGO4b, and OsAGO16 are involved in DNA methylation of target miRNAs, a process mediated by long miRNAs (48). Finally, the AGO1 homologs AGO1a, AGO1b, AGO1c, and AGO1d function in the miRNA pathway (49). Although AGO proteins might play roles in RNA-mediated gene silencing in rice, how they participate in PCD in anthers to affect male gametophyte development through DNA methylation is largely unknown.

Here, we performed a detailed functional characterization of *OsAGO2* in rice. *OsAGO2* was highly expressed in anthers before stage 12 during microspore development. Knockdown of *OsAGO2* led to the overaccumulation of ROS, leading to the early initiation of PCD, abnormal anther development, and reduced pollen fertility. Interestingly, we found that the knockdown of *OsAGO2* led to the up-regulation of *OsHXK1* expression and that OsAGO2 directly regulates the expression of *OsHXK1* via DNA methylation. Overexpression of *OsHXK1* led to the early initiation of tapetal degeneration and reduced pollen fertility, which is similar to the phenotypes of plants with knocked-down *OsAGO2* expression. These findings suggest that OsHXK1 positively regulates the appropriate production of ROS and proper timing of tapetal PCD through the epigenetic regulation of *OsAGO2* expression.

Results

Spatiotemporal Expression Pattern of *OsAGO2*. *OsAGO2* is a member of the AGO family, comprising 19 members in rice. *OsAGO2* is located on chromosome 4 and contains three exons and two introns. The full-length 3,473-bp cDNA clone of *OsAGO2* contains a 3,105-bp ORF encoding a 1,034 amino acid protein (NP_001053871) of 111 kDa. AGO family members can be divided into four groups, AGO1, AGO4, MEL1/AGO5, and ZIPPY/AGO7, according to their conserved domains (39, 43). OsAGO2 belongs to the ZIPPY/AGO7 clade and contains the PAZ and PIWI domains typical of AGO proteins. To explore the evolutionary relationships of AGO proteins in various species, we performed multiple sequence alignment of the amino acid sequences of the PAZ and PIWI domains of AGO2 in various species (*SI Appendix*, Fig. S1*A*) using Evolview (www.evolgenius.info/evolview/). Based on this phylogenetic analysis, AGO2 protein sequences are relatively conserved among plants.

To characterize the expression of *OsAGO2*, we measured its transcript levels in various tissues by qRT-PCR and β-glucuronidase (GUS) activity analysis. The cytological descriptions of different stages of rice anther development used in this study are based on those described by Zhang et al. (9). Strong expression of *OsAGO2* was detected in anthers before stage 12 during microspore development (*SI Appendix*, Fig. S2*A*). Analysis of GUS activity directed by the *OsAGO2* promoter revealed strong GUS staining in anthers from stages 4–11 (*SI Appendix*, Fig. S2*B*), confirming the expression patterns obtained by qRT-PCR. To further explore the spatial and temporal expression patterns of *OsAGO2* during anther development, we performed RNA in situ hybridization using WT plants. Strong in situ signals were observed in tapetal cells from stages 6–9 (*SI Appendix*, Fig. S2*C*). Signals were also detected in the epidermis (from stages 5–6), endothecium, meiocytes, and microspores from stages 5–9. As a negative control, hybridization with the *OsAGO2* sense probe did not produce any detectable signal. These results suggest that OsAGO2 might be involved in anther development in rice.

To investigate the subcellular localization of OsAGO2, we fused the yellow fluorescent protein (YFP) sequence to the C terminus of OsAGO2 and expressed the fusion protein (OsAGO2-YFP) under the control of the CaMV35S promoter. We transformed this construct into sheath protoplasts of Zhonghua11 (*O. sativa* L. ssp. *japonica*. cv. Zhonghua11, ZH11) and detected the localization of the YFP fusion protein in cytoplasm and nuclei based on the colocalization of YFP fluorescence and DAPI staining (*SI Appendix*, Fig. S1*B*). The presence of OsAGO2-YFP in the cytoplasm and nuclei was also verified by immunoblotting (*SI Appendix*, Fig. S1*C*). These results demonstrate that *OsAGO2* is highly expressed in tapetal cells and its encoded protein is mainly localized to the cytoplasm and nuclei.

Phenotypic Analysis of *OsAGO2* Knockdown Plants. To explore the function of OsAGO2 in tapetal cells, we constructed an *OsAGO2* antisense vector containing the gene-specific *OsAGO2* fragment driven by the native promoter and a CRISPR/Cas9 vector targeting the *OsAGO2* gene. We then transformed ZH11 calli with these two constructs (50, 51). Nine independent transgenic lines were obtained, including four antisense and five CRISPR/Cas9 lines (*SI Appendix*, Fig. S3 and Table S1). For each knockdown method, two lines that exhibited the lowest *OsAGO2* transcript levels in the T_1 generation (as determined by qRT-PCR) were selected for further study, and were named *ago2-1*, *ago2-2*, *Casago2-1*, and *Casago2-2* (Fig. 1*D*). There are two rice proteins (OsAGO2, OsAGO3) in the ZIPPY/AGO7 subfamily and they share high sequence similarity with each other. Because the PAZ and PIWI domains of OsAGO2 share high sequence similarity with those of OsAGO3 (*SI Appendix*, Fig. S1*A*), we also examined the expression levels of *OsAGO3* in *ago2-1*, *ago2-2*, *Casago2-1*, and *Casago2-2* plants by qRT-PCR. *OsAGO3* expression was not altered in the antisense or CRISPR/Cas9 mutants (*SI Appendix*, Fig. S4*A*). Therefore, our antisense and CRISPR/Cas9 systems caused considerable suppression of *OsAGO2* without having obvious effects on its highly similar homolog, *OsAGO3*.

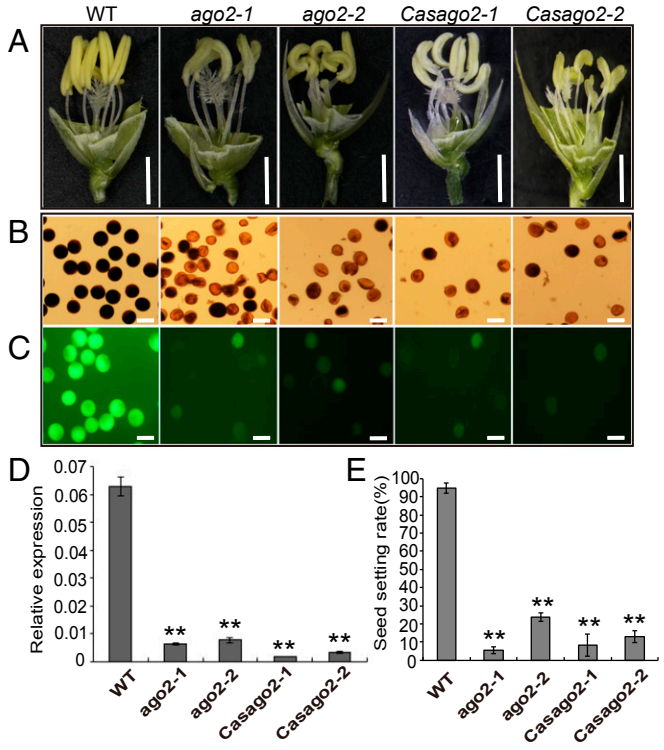

Fig. 1. Phenotypic comparison of the WT, *ago2-1*, *ago2-2*, *Casago2-1*, and *Casago2-2* plants. (*A*) WT, *ago2-1*, *ago2-2*, *Casago2-1*, and *Casago2-2* spikelets after removing the lemma and palea. (Scale bars, 2 mm.) (*B*) Staining of WT, *ago2-1*, *ago2-2*, *Casago2-1*, and *Casago2-2* pollen grains with I_2/KI solution. (Scale bars, 50 μm.) (*C*) FDA staining of WT, *ago2-1*, *ago2-2*, *Casago2-1*, and *Casago2-2* pollen. (Scale bars, 50 μm.) (*D*) qRT-PCR analysis of *OsAGO2* transcript in the WT, *ago2-1*, *ago2-2*, *Casago2-1*, and *Casago2-2* plants. Error bars indicate SD. (*E*) Comparison of the WT, *ago2-1*, *ago2-2*, *Casago2-1*, and *Casago2-2* panicles at the seed maturation stage showing seed-setting rate. $^{**}P < 0.01$. Each reaction represents three biological repeats.

These four antisense and CRISPR/Cas9 lines exhibited delayed growth (*SI Appendix*, Fig. S4*C*) and reduced fertility compared with WT, with shrunken, shortened stamens containing distorted pollen grains (Fig. 1*A*). The seed-setting rates of *ago2-1*, *ago2-2*, *Casago2-1*, and *Casago2-2* were 5.6%, 23.6%, 8.2% and 12.8%, respectively, which were greatly reduced compared with the rate of 95% observed in WT plants (Fig. 1*E* and *SI Appendix*, Fig. S4*D*). We also examined pollen viability by iodine/potassium iodide (I_2/KI) (Fig. 1*B*) and fluorescein diacetate (FDA) staining (Fig. 1*C*). The pollen grains of *ago2-1*, *ago2-2*, *Casago2-1*, and *Casago2-2* appeared lighter than WT when stained with I_2/KI (Fig. 1*B*), and very few were viable, in contrast to the almost full viability of WT pollen grains (Fig. 1*C*). Taken together, these results indicate that the knockdown of *OsAGO2* results in abnormal anther appearance, compromised pollen viability, and reduced seed development in rice.

Loss-of-Function of OsAGO2 Causes Defective Anther Development. To further examine the defects in anther development of *OsAGO2*-knockdown plants, we examined semithin sections of anthers by light microscopy. At stage 5 of anther development, no obvious differences were observed between *OsAGO2*-knockdown and WT plants (*SI Appendix*, Fig. S5). Compared with normal WT anther development (Fig. 2 *A–G*), in *OsAGO2*-knockdown plants, cytoplasm loosening and vacuolization were observed in microsporocytes and tapetum from stages 6–8 (Fig. 2 *A1–A4*, *B1–B4*, and *C1–C4*). At stage 9, the tapetum swelled severely, and irregular microspores were observed (Fig. 2 *D1–D4*). At stage 10, as the swollen, inward-growing tapetum enlarged, the microspores were squeezed into an irregular shape (Fig. 2 *E1–E4*). At stage 11, the anthers of knockdown plants showed diffuse vacuolation, and the microspores were distorted (Fig. 2 *F1–F4*). Until stage 12, the number of round microspores decreased, and some microspores developed abnormally, perhaps due to the reduced accumulation of starch and other materials (Fig. 2 *G1–G4*). These results indicate that *ago2-1*, *ago2-2*, *Casago2-1*, and *Casago2-2* anthers have defective microspores and tapetal cells, thus affecting pollen development.

To gain more insight into the defects of the tapetal cells of *ago2-1*, *ago2-2*, *Casago2-1*, and *Casago2-2* plants, we used transmission electron microscopy (TEM) to investigate the ultrastructural features of the tapetum. The results of TEM were consistent with the results of analysis of transverse sections by light microscopy (Fig. 3 and *SI Appendix*, Figs. S5 and S6). The anthers of *OsAGO2*-knockdown plants were considerably different from those of WT (Fig. 3 *A–D*). In mutant plants, the anthers showed more vacuoles around the nuclear periphery, and the tapetum remained loose and displayed numerous wavy shapes from stages 6–8 (Fig. 3 *A1–C1*, *A2–C2*, *A3–C3*, and *A4–C4* and *SI Appendix*, Fig. S6 *B–B2*, *C–C2*, *D–D2*, and *E–E2*). At stage 9, shrunken microspores and irregular tapetal cells with larger vacuoles were observed (Fig. 3 *D1–D4* and *SI Appendix*, Fig. S6 *B3*, *C3*, *D3*, and *E3*). At stages 10 and 11, the cytoplasm of the tapetum of knockdown plants remained loosened, with more peroxisomes and obvious mitochondria clearly visible (*SI Appendix*, Fig. S6 *B4*, *B5*, *C4*, *C5*, *D4*, *D5*, *E4*, *E5*, *F*, and *G*). These results support the finding that the early initiation of tapetal degradation occurs and the degradation process is abnormal in *ago2-1*, *ago2-2*, *Casago2-1*, and *Casago2-2* anthers.

Down-Regulation of *OsAGO2* Leads to ROS Overaccumulation and the Early Initiation of Tapetal PCD. PCD is an important feature of anther development in rice. In *OsAGO2*-knockdown anthers, abnormal degeneration of tapetal cell was observed (Figs. 2 and

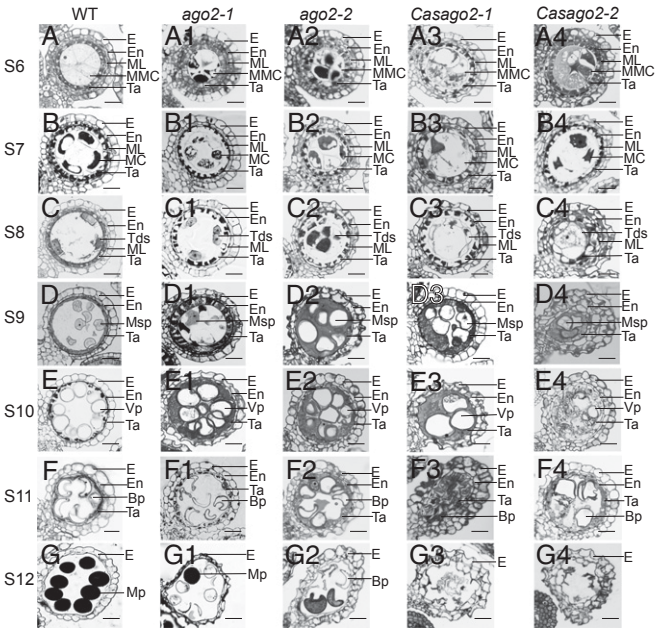

Fig. 2. Bright-field microscopy of transverse sections of anthers. Bright-field photomicrograph of transverse sections showing anther and microspore development in the WT (*A–G*), *ago2-1* (*A1–G1*), *ago2-2* (*A2–G2*), *Casago2-1* (*A3–G3*), and *Casago2-2* (*A4–G4*) from stage 6 to stage 12. Bp, bicellular pollen; E, epidermis; En, endothecium; MC, meiocyte; ML, middle layer; MMC, microspore mother cell; Mp, matured pollen; Msp, microspore parietal cell; Ta, tapetum; Tds, tetrads; VP, vacuolated microspore. (Scale bars, 25 μm.)

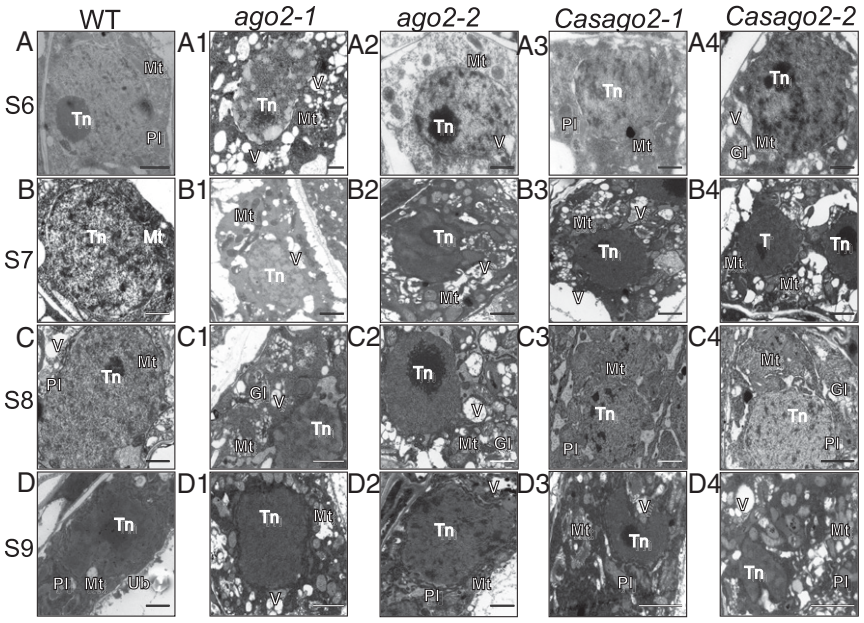

Fig. 3. TEM images of anthers. Higher magnification of the TEM observation showing tapetal cells of the WT (*A–D*), *ago2-1* (*A1–D1*), *ago2-2* (*A2–D2*), *Casago2-1* (*A3–D3*), and *Casago2-2* (*A4–D4*) from stage 6 to stage 9. Gl, golgiosome; Mt, mitochondrion; Pl, proplastid; Tn, tapetal nucleus; Ub, Ubisch bodies; V, vacuole. (Scale bars, 1 μm.)

3), likely due to PCD. To determine whether the altered *OsAGO2* expression in knockdown plants affects tapetal PCD, we examined DNA fragmentation in the plants using a TUNEL assay. In WT tapetal cells, TUNEL$^+$ signals were not detected at stages 6 or 7 (Fig. 4 *A* and *B*), began to appear at stage 8, were strongest at stage 9 (Fig. 4 *C* and *D*), and gradually weakened from stages 10–12 (Fig. 4 *E–G*). In contrast, in *ago2-1*, *ago2-2*, *Casago2-1*, and *Casago2-2* tapetal cells, TUNEL$^+$ signals were observed as early as stage 6 (Fig. 4 *A1–A4*), suggesting that tapetal PCD begins prematurely in *OsAGO2*-knockdown plants. The signals became increasingly stronger from stages 7–9 and peaked at stage 8 (Fig. 4 *B1–B4*, *C1–C4*, and *D1–D4*). Signals were still present at stages 10 and 11 and became weaker at stage 12 (Fig. 4 *E1–E4*, *F1–F4*, and *G1–G4*). TUNEL$^+$ signals were also detected in both the endothecium layer and microspores of these lines from stages 6–9 (Fig. 4 *A1–A4*, *B1–B4*, *C1–C4*, and *D1–D4*). These results indicate that PCD is initiated earlier in *OsAGO2*-knockdown anthers compared with WT.

ROS can induce PCD in plants (52, 53). We therefore measured ROS production in plants during anther development based on superoxide anion and hydrogen peroxide (H_2O_2) levels by nitro blue tetrazolium (NBT) and 2′, 7′-dichlorodihydrofluorescein diacetate (H_2DCF-DA) staining. Consistent with the results of the TUNEL assay, ROS levels in WT anthers were high at stages 8 and 9 and decreased at stage 10 (Fig. 5*A*). However, in *ago2-1* and *Casago2-1* anthers, high ROS levels were detected from stages 6–12 (Fig. 5 *B* and *C*). Histological analysis of anther sections revealed that superoxide anion was mainly localized to the tapetum and microspores (Fig. 5*E*). Measurement of H_2O_2 levels also revealed higher ROS level in *ago2-1* and *Casago2-1* vs. WT anthers from stages 8–12 (Fig. 5*F*). These results imply that downregulating or altering the expression of *OsAGO2* leads to the overaccumulation of ROS in anthers.

Characterization of *OsHXK1* as a Candidate Target Gene of OsAGO2. To identify target genes of OsAGO2, we performed microarray analysis of WT and *ago2-1* spikelets at stage 5. Because AGO proteins negatively regulate gene expression at the transcriptional or posttranscriptional levels (54), we focused on up-regulated genes in *ago2-1* plants. Fifty genes were found to be up-regulated (>twofold and $q < 0.05$ with a false discovery rate of 0.05%) in two replicate screenings. Among these 50 genes, *OsHXK1* (Os07g0446800) was up-regulated 2.96-fold in *ago2-1* anthers. Hexokinase (HXK) is an essential enzyme that phosphorylates glucose and fructose. In *Arabidopsis*, HXK1 is thought to contribute to the generation of ROS (55, 56). We reasoned that *OsHXK1* might be a target of OsAGO2.

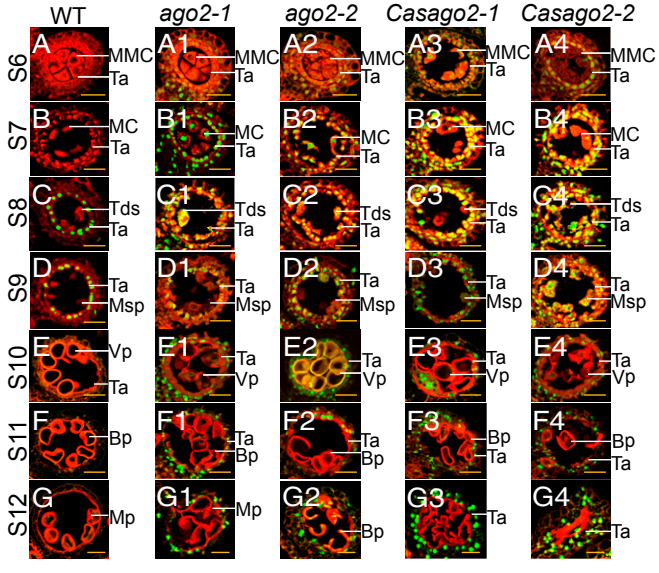

Fig. 4. Detection of DNA fragmentation by TUNEL assays of anthers. DNA fragment signals in WT (*A–G*), *ago2-1* (*A1–G1*), *ago2-2* (*A2–G2*), *Casago2-1* (*A3–G3*), and *Casago2-2* (*A4–G4*) anthers from stage 6 to stage 12. The red fluorescence results from staining of anthers with propidium iodide (PI) visualized by confocal laser-scanning microscopy; images are overlays of green fluorescence from TUNEL staining with PI staining. Bp, bicellular pollen; MC, meiocyte; MMC, microspore mother cell; MP, mature pollen; Msp, microspore parietal cell; Ta, tapetal cell; Tds, tetrads; VP, vacuolated microspore. (Scale bars, 20 μm.)

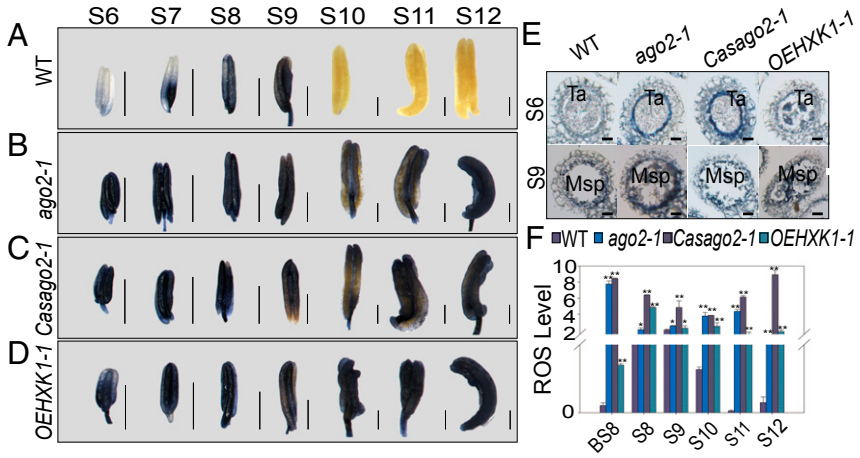

Fig. 5. Analyses of ROS in WT, *ago2-1*, *Casago2-1*, and *OEHXK1-1* anthers. (*A–D*) NBT staining of superoxide anion production from stage 6 to stage 12 in WT (*A*), *ago2-1* (*B*), *Casago2-1* (*C*), and *OEHXK1-1* (*D*) anthers. (Scale bars, 0.5 mm.) (*E*) NBT staining of anther sections in WT, *ago2-1*, *Casago2-1*, and *OEHXK1-1* anthers at stage 6 and at stage 9. (Scale bars, 25 μm.) Msp, microspore parietal cell; Ta, tapetal cell. (*F*) Relative quantification of ROS levels in WT, *ago2-1*, *Casago2-1*, and *OEHXK1-1* anthers at different stages based on H_2DCF-DA staining of ROS. *$0.01 < P < 0.05$. **$P < 0.01$. Error bars indicate SD. Each reaction represents three biological repeats.

To analyze the expression patterns of Os*HXK1*, we performed qRT-PCR using WT, *ago2-1*, and *Casago2-1* anthers. *OsHXK1* was expressed at extremely low levels during anther development in WT plants. In contrast, *OsHXK1* expression was significantly higher in *ago2-1* and *Casago2-1* plants, especially at stages 5–12 (*SI Appendix*, Fig. S7*A*). We also performed RNA in situ hybridization of WT, *ago2-1*, and *Casago2-1* anther sections. Consistent with the qRT-PCR results, in situ hybridization revealed that *OsHXK1* was expressed at significantly higher levels in *ago2-1* and *Casago2-1* tapetal cells than in WT at stages 8 and 10 (*SI Appendix*, Fig. S7*B*). OsHXK1 was mainly localized to the cytoplasm (*SI Appendix*, Fig. S7*C*). These results suggest that *OsHXK1*, which is up-regulated in *ago2-1* and *Casago2-1* anthers, is a target gene of OsAGO2.

Overexpression of *OsHXK1* Causes Defective Anther Development and Early Initiation of PCD. To determine whether increasing the expression of *OsHXK1* influences tapetum and pollen development, we constructed an *OsHXK1* overexpression vector and transferred it into ZH11 rice plants. Two independent transgenic lines were selected, which we named *OEHXK1-1* and *OEHXK1-2* (*SI Appendix*, Fig. S7*D* and Table S1). We examined the pollen viability in the plants by I_2/KI staining (*SI Appendix*, Fig. S7*E*). As shown in *SI Appendix*, Fig. S7*E*, ∼75% and 74% of the pollen grains from *OEHXK1-1* and *OEHXK1-2* plants were stained lighter than those of the WT, respectively, indicating that pollen viability was reduced in *OEHXK1-1* and *OEHXK1-2* plants. The seed-setting rates of *OEHXK1-1* and *OEHXK1-2* plants were 14.1% and 27%, respectively, which were greatly reduced compared with the rate of 94.7% in WT plants (*SI Appendix*, Fig. S7*F*). These results strongly indicate that increasing *OsHXK1* expression affects pollen fertility.

HXK1 possesses hexokinase catalytic activity in *Arabidopsis*, in which Gly^{109} and Ser^{182} are the key catalytic sites (55). To determine the relationship between OsHXK1 hexokinase catalytic activity and the altered phenotypes of plants, we generated three catalytically inactive overexpression lines (*OEHXK1D1*, *OEHXK1D3*, and *OEHXK1D8*). Based on the key catalytic sites in *Arabidopsis*, OsHXK1 was mutated at two active sites, $Gly^{109} \rightarrow Asp^{109}$ (G109D) and $Ser^{182} \rightarrow Ala^{182}$ (S182A) in these overexpression plants. These overexpression lines all displayed increased OsHXK1 expression and normal fertility, like WT plants (*SI Appendix*, Fig. S8). These results suggest that the catalytic activity of *OsHXK1* is necessary for the altered phenotypes in the overexpression lines.

To examine the characteristics of pollen abortion in *OEHXK1-1* and *OEHXK1-2* anthers, we examined transverse semithin anther sections by light microscopy (Fig. 6 *A–C*). *OEHXK1-1* and *OEHXK1-2* anthers were considerably different from WT anthers. The following abnormalities were observed: cytoplasm vacuolization, expanded tapetum, and irregular tetrads appeared (from stages 6–8); the tapetum swelled severely and began to form hill-like shapes on the inner surface (stage 9); and microspores were squeezed into irregular shapes and became distorted (stages 10–12). To determine the effect of overexpression of *OsHXK1* on tapetal PCD, we examined DNA fragmentation using the TUNEL assay (Fig. 6 *D–F*). Enhanced positive signals were observed in *OEHXK1-1* and *OEHXK1-2* tapetum from stages 6–12, when obvious signals were also present in microspores and other anther wall tissues (Fig. 6 *E* and *F*). These results suggest that overexpressing *OsHXK1* leads to early initiation of tapetal degeneration and subsequent pollen abortion. A ROS production assay also revealed that ROS levels increased in *OEHXK1-1* anthers from stages 6–12 (Fig. 5*D*). Similarly, ROS levels were higher in *OEHXK1-1* anthers than in WT anthers (Fig. 5 *E* and *F*). Microscopy of transverse semithin anther sections, TUNEL assays, and NBT and H_2DCF-DA assays showed that the characteristics of anther development in *OEHXK1-1* plants were similar to those in *OsAGO2*-knockdown plants. These results imply that overexpressing *OsHXK1* leads to the overaccumulation of ROS, thereby damaging the anthers in the Os*HXK1* overexpression lines. Therefore, it appears that OsHXK1 positively controls proper ROS production, the timing of tapetal PCD, and microspore development, with the phenotypes of *ago2-1*, *ago2-2*, *Casago2-1*, and *Casago2-2* plants similar to those of *OsHXK1* overexpression plants.

Changes in the Expression of Genes Involved in Tapetal PCD and ROS Production in *ago2-1* Anthers. Based on the early initiation of PCD in *ago2-1*, *ago2-2*, *Casago2-1*, and *Casago2-2* anthers, we reasoned that some genes critical for anther development might be affected in these plants. Therefore, we used qRT-PCR to examine the expression of nine genes involved in anther development, including *OsUDT1* (25), *OsTIP2* (26, 27), *OsTDR1* (10), *OsEAT1*/*DTD* (28, 29), *OsMYB80*/*OsMYB103* (20–22), *OsTGA10* (57, 58), *OsPTC1* (11), *OsMADS3* (15), and *OsDTC1* (59) (*SI*

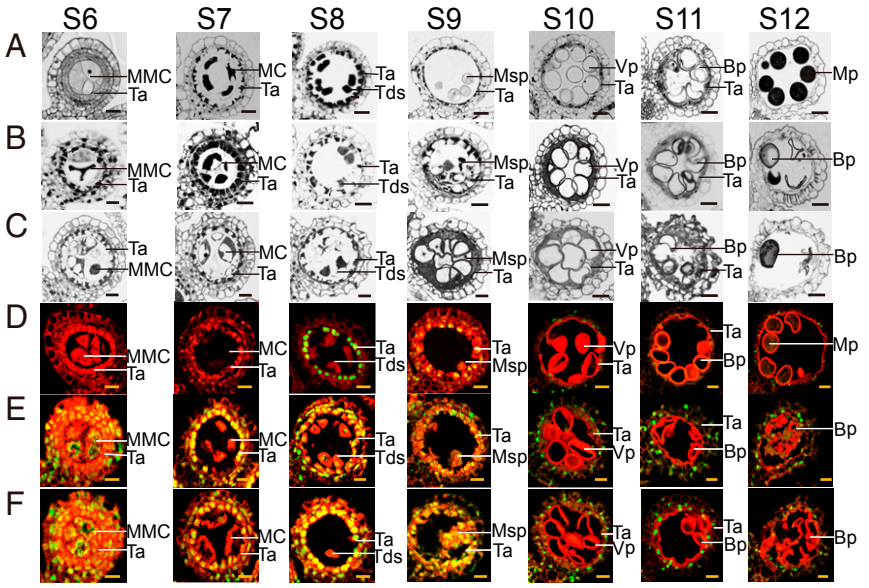

Fig. 6. Transverse section characterization and TUNEL analysis of *OEHXK1-1* and *OEHXK1-2* anthers. (*A–C*) The comparison of transverse section characterization in WT (*A*), *OEHXK1-1* (*B*), and *OEHXK1-2* (*C*). (*D–F*) DNA fragment signals in WT (*D*), *OEHXK1-1* (*E*), and *OEHXK1-2* (*F*) plants from stage 6 to stage 12. The red fluorescence results from staining of anthers with PI visualized by confocal laser scanning microscopy; images are overlays of green fluorescence from the TUNEL staining with PI staining. Bp, bicellular pollen; MC, meiocyte; MMC, microspore mother cell; MP, mature pollen; Msp, microspore parietal cell; Ta, tapetal cell; Tds, tetrads; VP, vacuolated microspore. (Scale bars, 20 μm.)

Appendix, Fig. S9). These genes encode bHLH, MYB, PHD-finger, and MADS box transcription factors. Six of these genes (*OsUDT1*, *OsTIP2*, *OsTDR1*, *OsEAT1/DTD*, *OsMYB80/OsMYB103*, and *OsTGA10*) were significantly down-regulated in *ago2-1* and *Casago2-1* anthers compared with WT anthers (*SI Appendix*, Fig. S9 *A–F*). These results suggest that OsAGO2 might mediate a pathway in the regulatory network for anther development.

Optimal ROS levels are required for tapetal PCD. Plant NADPH oxidase genes known as respiratory burst oxidase homolog (RBOH) genes play a role in ROS generation. The proper timing of tapetal PCD is ensured by a transcriptional network, including proper ROS patterns produced by RBOHs (53). The rice genome contains nine RBOH family members, including *OsRBOHa/OsNOX*, *OsRBOHb*, *OsRBOHc*, *OsRBOHd*, *OsRBOHe*, *OsRBOHf*, *OsRBOHg*, *OsRBOHh*, and *OsRBOHi*. To determine the reason for the increase in ROS levels in the mutants, we carried out qRT-PCR analysis to examine the expression levels of the *OsRBOH* genes. As shown in *SI Appendix*, Fig. S10 *A*, *B*, *D*, and *E*, the *OsRBOH* genes were expressed at higher levels from stages 5–12 in *ago2-1* and *Casago2-1* anthers compared with WT. These results suggest that the changes in the expression patterns of *OsRBOH* genes lead to increased ROS accumulation in *ago2-1* and *Casago2-1* anthers, which might serve as signaling molecules in tapetal PCD.

To investigate the relationship between OsAGO2 and Os*HXK1*, we analyzed the expression levels of the nine genes involved in anther development mentioned above in *OEHXK1-1* plants. All nine genes were also down-regulated in *OEHXK1-1* plants vs. WT (*SI Appendix*, Fig. S9). Furthermore, the expression levels of the *OsRBOHs* in *OEHXK1-1* plants were also higher from stages 5–10 compared with WT anthers (*SI Appendix*, Fig. S10). Therefore, several anther development-related and *OsRBOH* family genes exhibited changes in expression in *ago2-1* and *Casago2-1* anthers similar to those in *OEHXK1-1* anthers. These results suggest that OsAGO2 and OsHXK1 function in a similar regulatory pathway during anther development.

OsAGO2 Directly Regulates *OsHXK1* Expression via DNA Methylation. Because the phenotypes of *OEHXK1-1* plants were similar to those of *ago2-1* and *Casago2-1* plants, we reasoned that *OsHXK1* is directly regulated by OsAGO2. To investigate this hypothesis, we knocked down the expression of *OsHXK1* using CRISPR/Cas9 and RNA interference (RNAi) in plants in the *ago2-1* background. For each knockdown method, two lines were selected for further analysis (*A2CH1-1* and *A2CH1-2* for CRISPR/Cas9; *A2Hi-1* and *A2Hi-2* for RNAi) (*SI Appendix*, Table S1). The progeny plants showed normal growth and development, with decreased *OsHXK1* and *OsAGO2* expression compared with WT (*SI Appendix*, Fig. S11 *A* and *B*). Bisulfite sequencing revealed a similar reduction in methylation levels to those in *ago2-1* plants (*SI Appendix*, Fig. S11*C*). I_2/KI staining showed that pollen fertility was restored in the progeny plants (*SI Appendix*, Fig. S11 *D* and *E*). These results suggest that OsAGO2 and *OsHXK1* interact and that *OsHXK1* is regulated by OsAGO2.

Because *OsHXK1* is not targeted by any known rice miRNAs, it appears that OsAGO2 does not regulate *OsHXK1* at the posttranscriptional level. Through genomic sequence analysis, we found that *OsHXK1* contains a GC-rich promoter. Therefore, we hypothesized that epigenetic regulation, particularly DNA methylation, may be responsible for the relationship between OsAGO2 and *OsHXK1*. To explore the interaction of OsAGO2 with *OsHXK1*, we analyzed the methylation level in the promoter region of *OsHXK1* in *ago2-1* and *Casago2-1* plants. In plants, cytosine methylation primarily occurs in three sequence contexts: CG, CHG, and CHH (H = A, T, or C). To analyze the methylation status of *OsHXK1* in *ago2-1* and *Casago2-1* DNA, we performed a bisulfite conversion reaction using a sequence starting 2,000-bp upstream of the transcriptional start site of *OsHXK1*. In the *OsHXK1* promoter region, the levels of CG, CHG, and CHH methylation in spikelets were lower in *ago2-1* and *Casago2-1* plants than in WT plants (Fig. 7 *A* and *B*). We performed quantitative pyrosequencing to further assess the methylation pattern of the *OsHXK1* promoter in cytosine sites from −856 to −382 bp. Eight CG positions (from position 1 to position 8) in *ago2-1* and *Casago2-1* plants displayed lower CG

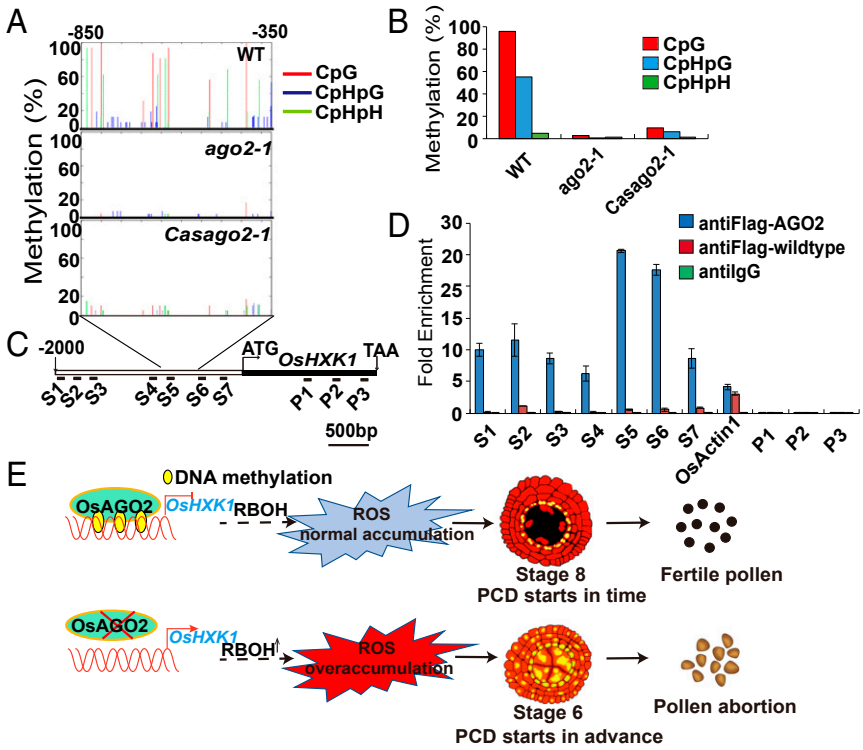

Fig. 7. OsAGO2 modulates *OsHXK1* expression through DNA methylation. (*A*) Distribution of cytosine DNA methylation in three contexts in 500-bp of the *OsHXK1* promoter region in WT, *ago2-1*, and *Casago2-1* plants as measured by bisulfite-sequencing. Sequencing data were analyzed using Kismeth software. CpG, red; CpHpG, blue; CpHpHp, green. (*B*) Methylation levels of CpG, CpHpG and CpHpHp in WT, *ago2-1*, and *Casago2-1* plants. (*C*) OsAGO2 bound to the *OsHXK1* promoter was measured by ChIP followed by qRT-PCR. (*D*) The fold-enrichments at the *OsHXK1* promoter by ChIP-qPCR conducted on stage 9–11 spikelets from the rice transgenic plants harboring *Ubi::FLAG-AGO2* constructs and WT plants. Negative control, anti-IgG (normal rabbit IgG antibody). S1–S7, seven different sequences in the promoter region of *OsHXK1*. P1–P3, three different sequences in the coding region of *OsHXK1*. Error bars indicate SD. Each reaction represents three biological replicates. (*E*) A proposed model for the OsAGO2-*OsHXK1* interaction that regulates anther ROS accumulation and tapetum PCD in rice. In this model, appropriate production of ROS and proper timing of tapetal PCD were controlled by OsHXK1, which was epigenetically regulated by OsAGO2.

methylation levels than those of WT plants (*SI Appendix*, Fig. S11*F*). These results suggest that OsAGO2 regulates the methylation status of the *OsHXK1* promoter.

To validate the binding of OsAGO2 to the *OsHXK1* promoter, we performed chromatin immunoprecipitation (ChIP) assays and analyzed the resulting purified ChIP DNA samples by qRT-PCR of specific regions at the *OsHXK1* promoter. Four DNA sequences (S2, S5, S6, and S7) were enriched by OsAGO2 when using an anti-FLAG antibody. However, sequences P1 to P3 lacking OsAGO2-binding sequences did not associate with OsAGO2 (Fig. 7 *C* and *D*). These results suggest that OsAGO2 binds to the *OsHXK1* promoter and directly regulates its expression via DNA methylation, thereby ensuring proper PCD and pollen development.

We propose a model to describe the function of OsAGO2 in rice pollen development, as shown in Fig. 7*E*. According to this model, OsHXK1 is an important regulator of ROS production and PCD in tapetal cells. OsAGO2 controls *OsHXK1* expression through methylation of its promoter, thereby ensuring the proper timing of tapetal PCD and normal pollen fertility. Our results reveal a regulatory pathway for pollen development in rice.

Discussion

OsAGO2 Is a Critical Regulator of Tapetum Development. Male reproductive development is a key step in determining grain yield and production in rice. The male gametophyte developmental process is broadly conserved across angiosperms. Anther development is a highly precise, complex process involving diverse gene regulatory pathways. It is important to uncover the gene regulatory networks that function during tapetum differentiation and PCD. Several genes have been shown to be associated with tapetal function and pollen development in rice (5, 7, 9), including *OsUDT1*/*bHLH164*, *OsTDR1*/*bHLH5*, *OsTIP2*/*bHLH142*, *OsEAT1*/*DTD1*/*bHLH141*, *OsDTC1*, *OsMYB80*/*OsMYB103*, *OsPTC1*, and *OsMADS3* (10, 11, 15, 25–28, 59). Among these, *OsTDR1* controls tapetum development and degeneration (10). *OsUDT1* plays a crucial role in the differentiation of secondary parietal cells to mature tapetal cells (25). *OsTIP2* regulates tapetal PCD and pollen wall development (26, 27). *OsDTC1* also acts as a key regulator of tapetal PCD through the inhibition of a ROS scavenger (59). *OsMYB80*/*OsMYB103* is involved in PCD in the tapetum, thereby influencing the late stage of anther development (20, 22). *OsPTC1* regulates tapetal PCD and pollen development (11). The absence of these genes can lead to abnormal tapetal PCD and male sterility. In the present study, we found that Os*AGO2* is highly expressed in rice tapetal cells from stages 5–11. Down-regulation of *OsAGO2* led to excessive ROS accumulation, which triggered PCD of tapetal cells. The PCD patterns were also found to be altered in these lines, with early initiation of PCD at stage 6 accompanied by DNA fragmentation in other cell layers.

The altered ROS accumulation and PCD patterns in *ago2-1*, *ago2-2*, *Casago2-1*, and *Casago2-2* anthers suggested that some genes critical for anther development might be affected in these lines. We therefore analyzed the transcript levels of six anther development-related genes, including *OsUDT1*, *OsTIP2*, *OsTDR1*, *OsEAT1*, *OsMYB80*/*OsMYB103*, and *OsTGA10*. Most of these genes are factors in the anther development regulatory networks in rice. The transcript levels of these six genes were markedly lower in *ago2-1* and *Casago2-1* anthers than in WT. In

WT plants, the expression of these tapetum-specific genes terminates at stage 12. However, their expression was completely suppressed in *ago2-1* and *Casago2-1* anthers. In previous studies, the mutations of these genes led to delayed tapetal PCD (10, 20, 22, 25–29, 57, 58). However, we demonstrated that knocked down *OsAGO2* expression led to the early initiation of tapetal PCD, suggesting that the process of *OsAGO2*-mediated tapetal PCD might be different from that of the genes mentioned above.

Notably, although tapetal degradation began earlier in the knockdown plants, the degradation process was similar to that of WT plants and continued until stage 12. A similar phenomenon was also observed in studies of photoperiod-sensitive male sterility in rice (37, 60–62). Perhaps different mechanisms control PCD initiation and tapetal degradation. Normal tapetal degradation is regulated and coordinated by many other genes. Although altered *OsAGO2* expression led to the early initiation of PCD, the degradation process was not affected in tapetal cells of the *OsAGO2* mutants due to the down-regulation of various genes, such as *OsUDT1*, *OsTIP2*, *OsTDR1*, *OsEAT1*, *OsMYB80*/*OsMYB103*, and *OsTGA10*.

OsHXK1 Is a Critical Regulator of ROS Production and PCD in the Tapetum. Tapetal cells undergo PCD during the late stages of anther development. The correct timing and appropriate regulation of tapetal PCD are essential for pollen development and plant reproduction. Premature or delayed tapetal PCD and cellular degeneration can lead to male sterility (10, 11). In the present study, PCD was initiated early in *OEHXK1-1* and *OEHXK1-2* anthers. Enhanced TUNEL$^+$ signals were observed in the tapetum of these lines from stages 6–10. In addition to tapetal cells, strong TUNEL$^+$ signals were also detected in microspores and anther wall layers, causing the abnormal timing and tissue-specificity of PCD. These results suggest that OsHXK1 regulates tapetal PCD. Interestingly, HXK1 is also involved in regulating senescence and PCD in *Arabidopsis* (55, 56). These findings indicate that the regulatory patterns of tapetal PCD by OsHXK1 are conserved in plants.

During anther development, ROS production plays a role in regulating tapetal PCD, but how ROS regulate tapetal development remains unclear. Plant NADPH oxidase, also known as RBOH, is an important generator of ROS (63–67). In *Arabidopsis*, RBOH is critical for tapetal PCD (63). Several studies have shown that MAP kinase directly regulates the expression of RBOH genes (68, 69). Here, we showed that the production of ROS, particularly superoxide anion, increased from stages 6–12 and that the expression levels of RBOH genes increased from stages 5–10 in *OEHXK1-1* anthers. The similar changes in RBOH gene expression and ROS content suggest that RBOH may be necessary for ROS-dependent signal transduction in *OEHXK1-1* and *OEHXK1-2* anthers. These findings also suggest that OsHXK1 might regulate *OsRBOH* gene expression in an unknown manner, thereby controlling ROS production.

Our findings suggest that overexpressing *OsHXK1* causes increased *OsRBOH* gene expression and the overaccumulation of ROS in *OEHXK1-1* and *OEHXK1-2* anthers, leading to oxidative damage, the premature initiation of PCD and pollen abortion. Thus, it appears that OsHXK1 controls the proper timing of tapetal PCD and microspore development.

OsAGO2 Directly Suppresses *OsHXK1* Expression Through an Epigenetic Pathway. DNA methylation, especially cytosine methylation, is widely present in plants. DNA methylation occurs almost exclusively at cytosines in CpG dinucleotides, leading to the suppression of gene expression. AGO proteins play essential roles in gene-silencing pathways guided by small RNAs (70–72). One strand of these small RNAs is then preferentially loaded onto the AGO protein to form an RNA-induced silencing complex. Several 24-nt miRNAs were found to direct DNA methylation and affect epigenetic silencing of male gametophyte development in plants. In *Arabidopsis*, AGO proteins AGO4, AGO6, and AGO9 are involved in RNA-directed DNA methylation (70). In rice, OsAGO4 and OsAGO6 are both required for DNA methylation at most of their target loci (42). Although several studies of DNA methylation have been conducted, most have involved analysis at the whole-genome level rather than at specific genes (73). To determine if *OsHXK1* gene expression is associated with its DNA methylation state, we performed bisulfite sequencing analysis and ChIP assays of the *OsHXK1* promoter region. When we down-regulated the expression of *OsHXK1* in *OsAGO2*-knockdown plants, the normal phenotype was restored, suggesting that *OsHXK1* is directly regulated by OsAGO2. In *ago2-1* and *Casago2-1* anthers, eight CG positions in the *OsHXK1* promoter had lower methylation levels compared with WT, as determined by bisulfite sequencing analysis. The ChIP assay showed that OsAGO2 binds to the promoter of *OsHXK1*. We propose that *OsHXK1* expression is directly regulated epigenetically by DNA methylation-mediated OsAGO2-induced gene silencing, along with altered ROS production, which is modulated via an *OsHXK1*-dependent pathway.

In addition, AGO18b interacts with miR166 and regulates spikelet quantity and meiosis in maize (71). In rice, OsMEL1, which is essential for sporogenesis in anthers, was recently shown to recruit 21-nt phased small-interfering RNAs and function in the modification of histone H3 (47, 72). We hypothesize that the binding of OsAGO2 with the *OsHXK1* promoter and their interaction might function in a ROS accumulation and anther development regulatory network through DNA methylation, ensuring the proper timing of tapetal PCD and normal pollen fertility. Our findings suggest that DNA methylation in the CpG context may constitute an epigenetic modification in response to ROS accumulation in rice during anther development.

ROS Are Required for PCD Initiation and Inhibited Tapetal Degradation. We observed abnormal tapetal degradation in plants with down-regulated *OsAGO2* expression and plants with up-regulated *OsHXK1* expression. We compared the results of TUNEL analysis and cytological observation and found that the initiation of tapetal PCD was significantly advanced in these lines, while tapetal cell degradation was significantly delayed. In fact, similar phenomena were observed in other studies. In an *Arabidopsis MYB80* mutant, TUNEL signals in anthers appeared early (stages 9–13), whereas they were detected from stages 10–12 in WT plants (22). In *OsDEX1* rice mutants, TUNEL signals appeared early (stage 7) and continued to stage 8a, with persistent tapetum observed at stage 11. In contrast, in WT plants, TUNEL signals appeared at stage 8b and were detected until stage 9, and tapetal degradation was completed at stage 11 (74). Based on these results, tapetal degradation can be divided into two stages: PCD initiation and execution. Different signals and pathways are involved in the initiation and execution of PCD, causing the execution phase to appear after the initiation phase. The precise timing of these two phases is crucial for pollen development. The appearance of TUNEL signals indicates the initiation of tapetum degradation. However, the earlier initiation process observed in the mutant and transgenic lines examined in the present study does not imply that the execution process is accelerated in these plants.

ROS production is a key component of PCD initiation and execution. In *Arabidopsis*, loss-of-function of RBOHE resulted in the delayed appearance of TUNEL signals, while the overexpression of RBOHE resulted in increased ROS accumulation and both the earlier appearance and delayed disappearance of TUNEL signals (63). In WT rice plants, ROS began to accumulate at stage 8, reached a peak at stage 9, and were maintained at low levels following a sharp decline. At the same time, TUNEL signals emerged at stage 8 and disappeared at stage 10, while tapetal cells were completely degraded at stage 12. However, in *dtc1* mutant plants, ROS accumulation decreased without any apparent peaks.

There were no TUNEL signals at any stage, and tapetum degradation was delayed (59). Furthermore, there were no obvious differences in ROS accumulation or tapetum degradation between *MADS3* mutants and WT plants before stage 9. Tapetum cells were completely degraded at stage 11 in WT plants, while they were still observed at stage 12 in mutant plants (15). In the present study, ROS were maintained at high levels in anthers at different stages of pollen development in plants with down-regulated *OsAGO2* expression, as well as plants overexpressing *OsHXK1*, causing TUNEL signals to appear in advance and delaying tapetum degradation. These results indicate that high ROS levels during early anther development are required for tapetum degradation. The rapid reduction of ROS levels after the initiation of PCD is also essential for normal tapetum degradation.

Methods

Plant Materials and Growth Conditions. All transgenic and WT rice plants (*O. sativa* ssp. *japonica* cv. Zhonghua11, ZH11) used in this study were grown in the paddy field, and named *ago2-1*, *ago2-2*, Cas*ago2-1*, Cas*ago2-2*, *OEHXK1-1*, and *OEHXK1-2*.

Characterization of Transgenic Plant Phenotypes. Anthers from different developmental stages were collected and confirmed by examining semithin sections (10). TEM was performed as described in Li et al. (10). Anthers from different developmental stages, as defined by Zhang et al. (9), were collected. Pollen viability was analyzed by 1% I_2/KI staining. FDA staining of pollen was performed according to a previous study (74).

Vector Construction and Plant Transformation. To construct the *OsAGO2* antisense vector, an ∼300-bp reverse fragment of the *OsAGO2* cDNA sequence driven by its native promoter (∼2.3 kb) was inserted into the modified pCAMBIA1300 vector (50). To construct the *OsHXK1* overexpression vector, a 1,497-bp fragment of the *OsHXK1* cDNA sequence driven by the *Ubiquitin* promoter was inserted into the pYLox vector (75). To construct the RNAi vector for *OsHXK1*, an ∼300-bp fragment of the cDNA sequence was inserted into the pYLRNAi vector (76). To generate the inactive *OsHXK1* mutants, the 109th glycine (Gly^{109}) and 182nd serine (Ser^{182}) were mutated to asparagine (Asp^{109}) and alanine (Ala^{182}), respectively. The WT cDNA sequence was used as a template for PCR amplification. These oligonucleotides create nucleotide substitutions to induce amino acid changes. The mutagenized cDNAs were cloned into the pYLox vector as previously described (75). To construct the *ProAGO2::GUS* vector, the *OsAGO2* native promoter was inserted into the pCAMBIA1300G vector (50). To generate the CRISPR/Cas9 vector, the *OsAGO2* and *OsHXK1* target sequences were constructed using pYLgRNA-OsU6 and pYLgRNA-OsU3, as previously described (77). To generate the *35S::YFP-OsAGO2* and *35S::YFP-OsHXK1* vectors, full-length *OsAGO2* and *OsHXK1* cDNAs were amplified and fused with the N terminus of YFP in the pUC18 vector under the control of the Cauliflower mosaic virus (CaMV) 35S promoter (78). For the *Ubi::FLAG-AGO2* construct, full-length *OsAGO2* cDNA was amplified and fused with the N terminus of FLAG in the pYLox vector driven by the *Ubiquitin* promoter (76).

All constructs were confirmed by sequencing, introduced into *Agrobacterium tumefaciens* EHA105 cells and transformed into ZH11 by *Agrobacterium*-mediated transformation (50, 51). All primers used for vector construction are listed in *SI Appendix*, Table S3.

qRT-PCR Assay and Expression Analysis. RT-PCR and quantitative PCR were performed as previously described (74). Primers used for qRT-PCR analysis are listed in *SI Appendix*, Table S3.

In Situ Hybridization. Anthers from fresh young panicles of different developmental stages were immediately fixed, embedded in paraffin (Sigma-Aldrich), and sectioned to 5- to 7-μm thickness. Hybridization and immunological detection were performed as previously described (79).

Phylogenetic Analysis. Phylogenetic analysis of AGO2 from various eukaryotes was performed using the maximum-likelihood method. The best-fit models of evolution for the amino acid were selected following the Akaike Information Criterion with Prot Test server 2.4 (80). Phylogenetic analyses of rice and *Arabidopsis* AGO proteins were subsequently performed using the maximum-likelihood method with RaxML 8.1.5 with 1,000 bootstrap replicates on the WAG+I+G+F ≥ JTT+I+G+F -1 model (81). The phylogenetic trees were drawn using Evolview (www.evolgenius.info/evolview/) (82). The accession numbers of proteins used in the phylogenetic analysis are listed in *SI Appendix*, Table S2.

Subcellular Localization. For transient expression, protoplasts were isolated from the leaf sheaths of rice plants as described previously (83). $OsRNaseZ^{S1}$ and Anti-Histone H3 Antibody (Merck Millipore) were selected as the cytoplasmic and nuclear protein controls, respectively (61).

TUNEL Assay. Anther samples were collected at different developmental stages. The TUNEL assay was performed as described (10) using a TUNEL kit (DeadEnd Fluorometric TUNEL system; Promega) according to the manufacturer's instructions.

Microarray Analysis. RNA purification and Affymetrix microarray hybridization were performed by the Capital Bio Corporation (www.capitalbio.com).

Bisulfite Sequencing. The PCR products were size-excluded and purified. The purified products were cloned into the pMD18-T vector using a pMD18-T Vector Cloning kit (Takara). For each region, at least 12 individual clones were sequenced, and the sequencing data were analyzed using Kismeth software (katahdin.mssm.edu/kismeth/revpage.pl) (84).

ChIP-qPCR Analysis. ChIP assays were performed as described previously (85) with minor modifications. The details are provided in *SI Appendix, Materials and Methods*.

Histochemical Analysis. Histochemical analysis of GUS activity was performed as previously described (86).

Measurement of ROS Levels. The superoxide anion radical content of anthers at various developmental stages was assayed by NBT staining as described previously (10, 15, 20, 63).

Accession Numbers. Sequence data from this article can be found in the Rice Annotation Project (https://rapdb.dna.affrc.go.jp/). *OsAGO2*, *OsHXK1*, and *OsActin1* are listed under the following GenBank accession nos: *OsAGO2* (Os04g0615700), *OsHXK1* (Os07g0446800) and *OsActin1* (Os10g0510000). The tapetal genes include *OsUDT1* (Os07g0549600), *OsTIP2* (Os01g0293100), *OsTDR1* (Os02g0120500), *OsEAT1* (Os04g0599300), *OsMYB80/OsMYB103* (Os04g0470600), *OsTGA10* (Os09g0489500), *OsPTC1* (Os09g0449000), *OsMADS3* (Os01g0201700), and *OsDTC1* (Os07g0540366). The *OsRBOH* genes include *OsRBOHa/OsNOX* (Os01g0734200), *OsRBOHb* (Os01g0360200), *OsRBOHc* (Os05g0528000), *OsRBOHd* (Os05g0465800), *OsRBOHe* (Os01g0835500), *OsRBOHf* (Os08g0453700), *OsRBOHg* (Os09g0438000), *OsRBOHh* (Os12g0541300), and *OsRBOHi* (Os11g0537400).

ACKNOWLEDGMENTS. This work was supported by Genetically Modified Breeding Major Projects (Grant 2016ZX08001-004), National Basic Research Program of China (Grant 2016YFD0100405), and the National Natural Science Foundation of China (Grants 31871231, 31371225, and 30800596).

1. Zhong XH, Peng SB, Wang F, Huang NR (2004) Using heterosis and hybrid rice to increase yield potential in China. Rice is life: Scientific perspectives for the 21st century. *Proceedings of the World Rice Research Conference* (International Rice Research Institute, Los Baños, Philippines).
2. Arshad MS, et al. (2017) Thermal stress impacts reproductive development and grain yield in rice. *Plant Physiol Biochem* 115:57–72.
3. De Storme N, Geelen D (2014) The impact of environmental stress on male reproductive development in plants: Biological processes and molecular mechanisms. *Plant Cell Environ* 37:1–18.
4. Kang H, et al. (2016) Overexpression of wheat ubiquitin gene, Ta-Ub2, improves abiotic stress tolerance of *Brachypodium distachyon*. *Plant Sci* 248:102–115.
5. Zhang DB, Wilson ZA (2009) Stamen specification and anther development in rice. *Chin Sci Bull* 54:2342–2353.
6. Wilson ZA, Zhang DB (2009) From *Arabidopsis* to rice: Pathways in pollen development. *J Exp Bot* 60:1479–1492.
7. Zhang D, Yang L (2014) Specification of tapetum and microsporocyte cells within the anther. *Curr Opin Plant Biol* 17:49–55.
8. Sanders PM, et al. (1999) Anther developmental defects in *Arabidopsis thaliana* male-sterile mutants. *Sex Plant Reprod* 11:297–322.
9. Zhang D, Luo X, Zhu L (2011) Cytological analysis and genetic control of rice anther development. *J Genet Genomics* 38:379–390.
10. Li N, et al. (2006) The rice tapetum degeneration retardation gene is required for tapetum degradation and anther development. *Plant Cell* 18:2999–3014.
11. Li H, et al. (2011) PERSISTENT TAPETAL CELL1 encodes a PHD-finger protein that is required for tapetal cell death and pollen development in rice. *Plant Physiol* 156:615–630.
12. Parish RW, Li SF (2010) Death of a tapetum: A programme of developmental altruism. *Plant Sci* 178:73–89.

13. Pacini E (1997) Tapetum character states: Analytical keys for tapetum types and activities. *Can J Bot* 75:1448–1459.
14. Hsieh K, Huang AHC (2007) Tapetosomes in *Brassica* tapetum accumulate endoplasmic reticulum-derived flavonoids and alkanes for delivery to the pollen surface. *Plant Cell* 19:582–596.
15. Hu L, et al. (2011) Rice MADS3 regulates ROS homeostasis during late anther development. *Plant Cell* 23:515–533.
16. Luo D, et al. (2013) A detrimental mitochondrial-nuclear interaction causes cytoplasmic male sterility in rice. *Nat Genet* 45:573–577.
17. Sorensen AM, et al. (2003) The *Arabidopsis* ABORTED MICROSPORES (AMS) gene encodes a MYC class transcription factor. *Plant J* 33:413–423.
18. Zhang W, et al. (2006) Regulation of *Arabidopsis* tapetum development and function by DYSFUNCTIONAL TAPETUM1 (DYT1) encoding a putative bHLH transcription factor. *Development* 133:3085–3095.
19. Zhu J, et al. (2008) Defective in Tapetal development and function 1 is essential for anther development and tapetal function for microspore maturation in *Arabidopsis*. *Plant J* 55:266–277.
20. Zhang ZB, et al. (2007) Transcription factor AtMYB103 is required for anther development by regulating tapetum development, callose dissolution and exine formation in *Arabidopsis*. *Plant J* 52:528–538.
21. Zhu J, et al. (2010) AtMYB103 is a crucial regulator of several pathways affecting *Arabidopsis* anther development. *Sci China Life Sci* 53:1112–1122.
22. Phan HA, Iacuone S, Li SF, Parish RW (2011) The MYB80 transcription factor is required for pollen development and the regulation of tapetal programmed cell death in *Arabidopsis thaliana*. *Plant Cell* 23:2209–2224.
23. Yang WC, Ye D, Xu J, Sundaresan V (1999) The SPOROCYTELESS gene of *Arabidopsis* is required for initiation of sporogenesis and encodes a novel nuclear protein. *Genes Dev* 13:2108–2117.
24. Thorstensen T, et al. (2008) The Arabidopsis SET-domain protein ASHR3 is involved in stamen development and interacts with the bHLH transcription factor ABORTED MICROSPORES (AMS). *Plant Mol Biol* 66:47–59.
25. Jung KH, et al. (2005) Rice Undeveloped Tapetum1 is a major regulator of early tapetum development. *Plant Cell* 17:2705–2722.
26. Fu Z, et al. (2014) The rice basic helix-loop-helix transcription factor TDR INTERACTING PROTEIN2 is a central switch in early anther development. *Plant Cell* 26:1512–1524.
27. Ko SS, et al. (2014) The bHLH142 transcription factor coordinates with TDR1 to modulate the expression of EAT1 and regulate pollen development in rice. *Plant Cell* 26:2486–2504.
28. Niu N, et al. (2013) EAT1 promotes tapetal cell death by regulating aspartic proteases during male reproductive development in rice. *Nat Commun* 4:1445.
29. Ji C, et al. (2013) A novel rice bHLH transcription factor, DTD, acts coordinately with TDR in controlling tapetum function and pollen development. *Mol Plant* 6:1715–1718.
30. Zhang S, Fang ZJ, Zhu J, Gao JF, Yang ZN (2010) OsMYB103 is required for rice anther development by regulating tapetum development and exine formation. *Chin Sci Bull* 55:3288–3297.
31. Phan HA, Li SF, Parish RW (2012) MYB80, a regulator of tapetal and pollen development, is functionally conserved in crops. *Plant Mol Biol* 78:171–183.
32. Pu CX, et al. (2017) The rice receptor-like kinases DWARF AND RUNTISH SPIKELET1 and 2 repress cell death and affect sugar utilization during reproductive development. *Plant Cell* 29:70–89.
33. Kota SK, Feil R (2010) Epigenetic transitions in germ cell development and meiosis. *Dev Cell* 19:675–686.
34. Solís MT, et al. (2014) Epigenetic changes accompany developmental programmed cell death in tapetum cells. *Plant Cell Physiol* 55:16–29.
35. Cao H, et al. (2015) Histone H2B monoubiquitination mediated by HISTONE MONOUBIQUITINATION1 and HISTONE MONOUBIQUITINATION2 is involved in anther development by regulating tapetum degradation-related genes in rice. *Plant Physiol* 168:1389–1405.
36. Solís MT, El-Tantawy AA, Cano V, Risueño MC, Testillano PS (2015) 5-Azacytidine promotes microspore embryogenesis initiation by decreasing global DNA methylation, but prevents subsequent embryo development in rapeseed and barley. *Front Plant Sci* 6:472.
37. Ding J, et al. (2012) A long noncoding RNA regulates photoperiod-sensitive male sterility, an essential component of hybrid rice. *Proc Natl Acad Sci USA* 109:2654–2659.
38. Hutvagner G, Simard MJ (2008) Argonaute proteins: Key players in RNA silencing. *Nat Rev Mol Cell Biol* 9:22–32.
39. Carmell MA, Xuan Z, Zhang MQ, Hannon GJ (2002) The Argonaute family: Tentacles that reach into RNAi, developmental control, stem cell maintenance, and tumorigenesis. *Genes Dev* 16:2733–2742.
40. Havecker ER, et al. (2010) The *Arabidopsis* RNA-directed DNA methylation argonautes functionally diverge based on their expression and interaction with target loci. *Plant Cell* 22:321–334.
41. Zilberman D, Cao X, Jacobsen SE (2003) ARGONAUTE4 control of locus-specific siRNA accumulation and DNA and histone methylation. *Science* 299:716–719.
42. Duan CG, et al. (2015) Specific but interdependent functions for *Arabidopsis* AGO4 and AGO6 in RNA-directed DNA methylation. *EMBO J* 34:581–592.
43. Zhang Z, Liu X, Guo X, Wang XJ, Zhang X (2016) *Arabidopsis* AGO3 predominantly recruits 24-nt small RNAs to regulate epigenetic silencing. *Nat Plants* 2:16049.
44. Eun C, et al. (2011) AGO6 functions in RNA-mediated transcriptional gene silencing in shoot and root meristems in *Arabidopsis thaliana*. *PLoS One* 6:e25730.
45. Kapoor M, et al. (2008) Genome-wide identification, organization and phylogenetic analysis of Dicer-like, Argonaute and RNA-dependent RNA Polymerase gene families and their expression analysis during reproductive development and stress in rice. *BMC Genomics* 9:451.
46. Wu J, et al. (2015) Viral-inducible Argonaute18 confers broad-spectrum virus resistance in rice by sequestering a host microRNA. *eLife* 4:e05733.
47. Nonomura K, et al. (2007) A germ cell specific gene of the ARGONAUTE family is essential for the progression of premeiotic mitosis and meiosis during sporogenesis in rice. *Plant Cell* 19:2583–2594.
48. Wu L, et al. (2010) DNA methylation mediated by a microRNA pathway. *Mol Cell* 38: 465–475.
49. Wu L, et al. (2009) Rice microRNA effector complexes and targets. *Plant Cell* 21:3421–3435.
50. Li J, et al. (2011) Expression of RNA-interference/antisense transgenes by the cognate promoters of target genes is a better gene-silencing strategy to study gene functions in rice. *PLoS One* 6:e17444.
51. Hiei Y, Ohta S, Komari T, Kumashiro T (1994) Efficient transformation of rice (*Oryza sativa* L.) mediated by *Agrobacterium* and sequence analysis of the boundaries of the T-DNA. *Plant J* 6:271–282.
52. Wiseman A (2006) p53 protein or BID protein select the route to either apoptosis (programmed cell death) or to cell cycle arrest opposing carcinogenesis after DNA damage by ROS. *Med Hypotheses* 67:296–299.
53. Doyle SM, Diamond M, McCabe PF (2010) Chloroplast and reactive oxygen species involvement in apoptotic-like programmed cell death in *Arabidopsis* suspension cultures. *J Exp Bot* 61:473–482.
54. Zhang H, Xia R, Meyers BC, Walbot V (2015) Evolution, functions, and mysteries of plant ARGONAUTE proteins. *Curr Opin Plant Biol* 27:84–90.
55. Moore B, et al. (2003) Role of the *Arabidopsis* glucose sensor HXK1 in nutrient, light, and hormonal signaling. *Science* 300:332–336.
56. Bruggeman Q, et al. (2015) Involvement of *Arabidopsis* hexokinase1 in cell death mediated by myo-inositol accumulation. *Plant Cell* 27:1801–1814.
57. Yang L, et al. (2016) Regulatory role of a receptor-like kinase in specifying anther cell identity. *Plant Physiol* 171:2085–2100.
58. Chen ZS, et al. (2018) Transcription factor OsTGA10 is a target of the MADS protein OsMADS8 and is required for tapetum development. *Plant Physiol* 176:819–835.
59. Yi J, et al. (2016) Defective tapetum cell death 1 (DTC1) regulates ROS levels by binding to metallothionein during tapetum degeneration. *Plant Physiol* 170:1611–1623.
60. Zhou H, et al. (2012) Photoperiod- and thermo-sensitive genic male sterility in rice are caused by a point mutation in a novel noncoding RNA that produces a small RNA. *Cell Res* 22:649–660.
61. Zhou H, et al. (2014) RNase Z(S1) processes UbL40 mRNAs and controls thermosensitive genic male sterility in rice. *Nat Commun* 5:4884.
62. Zhang H, et al. (2013) Mutation in CSA creates a new photoperiod-sensitive genic male sterile line applicable for hybrid rice seed production. *Proc Natl Acad Sci USA* 110:76–81.
63. Xie H-T, Wan Z-Y, Li S, Zhang Y (2014) Spatiotemporal production of reactive oxygen species by NADPH oxidase is critical for tapetal programmed cell death and pollen development in *Arabidopsis*. *Plant Cell* 26:2007–2023.
64. Yamauchi T, et al. (2017) An NADPH oxidase RBOH functions in rice roots during lysigenous aerenchyma formation under oxygen-deficient conditions. *Plant Cell* 29:775–790.
65. Kawasaki T, et al. (1999) The small GTP-binding protein rac is a regulator of cell death in plants. *Proc Natl Acad Sci USA* 96:10922–10926.
66. Sagi M, Fluhr R (2006) Production of reactive oxygen species by plant NADPH oxidases. *Plant Physiol* 141:336–340.
67. Wong HL, et al. (2007) Regulation of rice NADPH oxidase by binding of Rac GTPase to its N-terminal extension. *Plant Cell* 19:4022–4034.
68. Takahashi F, Mizoguchi T, Yoshida R, Ichimura K, Shinozaki K (2011) Calmodulin-dependent activation of MAP kinase for ROS homeostasis in *Arabidopsis*. *Mol Cell* 41:649–660.
69. Liu Y, He C (2017) A review of redox signaling and the control of MAP kinase pathway in plants. *Redox Biol* 11:192–204.
70. Qi Y, et al. (2006) Distinct catalytic and non-catalytic roles of ARGONAUTE4 in RNA-directed DNA methylation. *Nature* 443:1008–1012.
71. Sun W, et al. (2018) AGO18b negatively regulates determinacy of spikelet meristems on the tassel central spike in maize. *J Integr Plant Biol* 60:65–78.
72. Komiya R, et al. (2014) Rice germline-specific Argonaute MEL1 protein binds to phasiRNAs generated from more than 700 lincRNAs. *Plant J* 78:385–397.
73. He XJ, Chen T, Zhu JK (2011) Regulation and function of DNA methylation in plants and animals. *Cell Res* 21:442–465.
74. Matsumura H, et al. (2003) Overexpression of Bax inhibitor suppresses the fungal elicitor-induced cell death in rice (*Oryza sativa* L) cells. *Plant J* 33:425–434.
75. Yu L, et al. (2010) Glyoxylate rather than ascorbate is an efficient precursor for oxalate biosynthesis in rice. *J Exp Bot* 61:1625–1634.
76. Hu X, Liu Y-G (2006) The construction of RNAi vectors and the use for gene silencing in rice. *Mol Plant Breed* 4:621–626.
77. Ma X, et al. (2015) A robust CRISPR/Cas9 system for convenient, high-efficiency multiplex genome editing in monocot and dicot plants. *Mol Plant* 8:1274–1284.
78. Cormack BP, Valdivia RH, Falkow S (1996) FACS-optimized mutants of the green fluorescent protein (GFP). *Gene* 173:33–38.
79. Kouchi H, Hata S (1993) Isolation and characterization of novel nodulin cDNAs representing genes expressed at early stages of soybean nodule development. *Mol Gen Genet* 238:106–119.
80. Abascal F, Zardoya R, Posada D (2005) ProtTest: Selection of best-fit models of protein evolution. *Bioinformatics* 21:2104–2105.
81. Stamatakis A (2014) RAxML version 8: A tool for phylogenetic analysis and post-analysis of large phylogenies. *Bioinformatics* 30:1312–1313.
82. He Z, et al. (2016) Evolview v2: An online visualization and management tool for customized and annotated phylogenetic trees. *Nucleic Acids Res* 44:W236–W241.
83. Yang JW, et al. (2014) A novel co-immunoprecipitation protocol based on protoplast transient gene expression for studying protein-protein interactions in rice. *Plant Mol Biol Report* 32:153–161.
84. Gruntman E, et al. (2008) Kismeth: Analyzer of plant methylation states through bisulfite sequencing. *BMC Bioinformatics* 9:371.
85. Haring M, et al. (2007) Chromatin immunoprecipitation: Optimization, quantitative analysis and data normalization. *Plant Methods* 3:11.
86. Zhou LZ, et al. (2013) Protein S-ACYL Transferase10 is critical for development and salt tolerance in *Arabidopsis*. *Plant Cell* 25:1093–1107.